

Classification Study of WISE Infrared Sources: Identification of Candidate Asymptotic Giant Branch Stars

Xun Tu^{1,2} and Zhongxiang Wang¹

¹ Key Laboratory for Research in Galaxies and Cosmology and Shanghai Astronomical Observatory, Chinese Academy of Sciences, 80 Nandan Road, Shanghai 200030, China; wangzx@shao.ac.cn

² Graduate School of Chinese Academy of Sciences, No. 19A, Yuquan Road, Beijing 100049, China
 Received [year] [month] [day]; accepted [year] [month] [day]

Abstract In the WISE all-sky source catalogue there are 76 million mid-infrared (MIR) point sources that were detected at the first three WISE bands and have association with only one 2MASS near-IR source within $3''$. We search for their identifications in the SIMBAD database and find 3.2 million identified sources. Based on these known sources, we establish three criteria for selecting candidate AGB stars in the Galaxy, which are three defined occupation zones in a color-color diagram, Galactic latitude $|gb| \leq 20^\circ$, and “corrected” WISE third-band $W3_c \leq 11$. Applying these criteria to the WISE+2MASS sources, 1.37 million of them are selected. We analyze the WISE third-band $W3$ distribution of the selected sources, and further establish that $W3 \leq 8$ is required in order to exclude a large fraction of normal stars in them. We therefore find 0.47 million candidate AGB stars in our Galaxy from the WISE source catalogue. Using $W3_c$, we estimate their distances and derive their Galactic distributions. The candidates are generally located around the Galactic center uniformly, with 68% ($1-\sigma$) of them within approximately 8 kpc. We discuss that optical spectroscopy can be used to verify the C-rich AGB stars in our candidates, and they will be good targets for the LAMOST survey that is planned to start from fall of 2012.

Key words: stars: AGB and post-AGB — infrared: stars — stars: carbon

1 INTRODUCTION

Launched on 2009 December 14, the Wide-field Infrared Survey Explorer (WISE) surveyed the entire sky at four mid-infrared (MIR) bands 3.4, 4.6, 12 and 22 μm (hereafter named as W1, W2, W3, W4, respectively) over a year (Wright et al., 2010). Depending on the number of coverages of a sky region by WISE, the 5σ point source sensitivities reached were approximately better than 0.08, 0.11, 1 and 6 mJy in the four bands, respectively. The FWHMs of the averaged point spread function for WISE in the four bands were $6.1''$, $6.4''$, $6.5''$, and $12.0''$. The WISE all-sky images and source catalogue, released in 2012 March, contains over 563 million objects, having provided massive amount of information on MIR properties of many different types of celestial objects and their related phenomena (Wright et al., 2010). Given these, we have conducted analyses of the WISE sources for the purpose of identifying different classes of candidate objects among them. In this paper, we report our work on identification of candidate asymptotic giant branch (AGB) stars in the WISE catalogue.

AGB stars are low- to intermediate-mass ($1-8 M_\odot$) stars that have reached their final evolutionary stage (e.g., Herwig 2005). They have intense mass loss via a super-wind, and emission from the

ejected dust marks them as bright IR sources. Due to the so-called dredge-up process, O-rich or C-rich spectral features appear in emission from them, and these stars are called O-rich or C-rich AGB stars, respectively. The AGB stars, along with supernovae, are the major sources contributing to the interstellar medium (ISM) enrichment in galaxies (see, e.g., Matsuura et al. 2009). A survey of the Galactic AGB stars and studies of their properties will greatly help our understanding of chemical evolution of the ISM in the Galaxy. Previously Ishihara et al. (2011) have investigated the distributions of C-rich and O-rich AGB stars in our Galaxy using the AKARI MIR all-sky survey results (Murakami et al., 2007), but their results were limited by the relatively low sensitivities of the AKARI survey ($5\text{-}\sigma$ detection limits of 50 and 90 mJy at 9 and 18 μm respectively).

We describe our WISE data analyses in Section 2, which include WISE data selection, identification of WISE sources in the SIMBAD database, AGB star occupation zone determination in an IR color-color diagram based on the AGB stars known from the SIMBAD database, selection of a spatial distribution criterion for excluding extra-Galactic sources, and calculation of “corrected” W3 magnitudes $W3_c$ for estimation of distances of and further selection of AGB stars in the Galaxy. Results and further analyses of the found candidate AGB stars in the Galaxy are presented in Section 3. We discuss our results in Section 4.

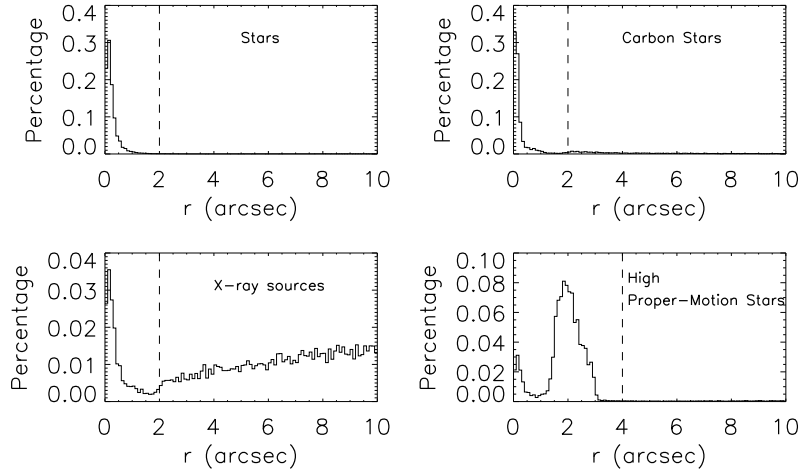


Fig. 1 Examples of the distribution of separation distances between WISE and SIMBAD sources.

2 DATA ANALYSIS

2.1 WISE Data

The WISE all-sky release source catalogue was downloaded from the NASA/IPAC infrared science archive (IRSA). The catalogue mainly contains positions and photometry and uncertainties in the four WISE bands for the sources detected by WISE. The positions were calibrated to the 2MASS point source catalogue, thus generally having an accuracy of $\sim 0.2''$ on each axis. Both profile-fitting and aperture photometry were performed to measure brightnesses of the WISE sources; we used the measurements from profile-fitting photometry in this work. The detailed description of the data analyses and products can be found in the WISE All-Sky Release Explanatory Supplement¹.

¹ <http://wise2.ipac.caltech.edu/docs/release/allsky/expsup>

Table 1 Numbers of IR Sources identified in the SIMBAD database

Class	Number ($r \leq 10''$)	Number ($r \leq 2''$)	Percent ($r \leq 2''$)
Star	2512531	2455250	—
Total	886300	748815	100
Galaxy	348533	325390	43
IR	78617	28305	3.8
*inCl	63327	57473	7.7
PM*	56281	54441	7.3
GinCl	34787	32568	4.3
*in**	29024	26199	3.5
V*	28764	25167	3.4
LPV*	26188	24661	3.3
Radio	23930	10509	1.4
semi-regV*	14819	14539	1.9
QSO	14640	13311	1.8
X	14405	3353	0.45
GinGroup	13297	12927	1.7
C*	12516	11039	1.5
**	8555	7820	1.0
Mira	8422	8227	1.1
low-mass*	8420	7896	1.1
Em*	6892	5529	0.74
RRLyr	6528	3260	0.44
Seyfert_1	6074	5883	0.79
EmG	5942	5658	0.76
*inAssoc	5345	4676	0.62
Candidate_YSO	5218	4175	0.56
PulsV*	3952	3855	0.51
AGN	3627	3500	0.47
EB*Algol	3521	3274	0.44
Seyfert_2	3408	3311	0.44
Candidate_AGB*	3339	3038	0.41
YSO	3230	2653	0.35
RGB*	3020	2864	0.38
EB*	3020	1493	0.20
RadioG	2798	2693	0.36
LSB_G	2669	2488	0.33
QSO_Candidate	2280	1883	0.25
EB*WUMa	1704	1477	0.20
UV	1613	583	0.078
pMS*	1601	1536	0.21
Cepheid	1452	997	0.13
deltaCep	1432	1220	0.16
PN	1421	786	0.10
Orion_V*	1305	1282	0.17
TTau*	1296	1229	0.16
ClG	1277	670	0.089
Be*	1270	1229	0.16
AGB*	1257	1207	0.16
GinPair	1244	1211	0.16
*inNeb	1239	719	0.096
Candidate_HB*	1206	1177	0.16
HB*	1114	1039	0.14
Flare*	1062	1002	0.13
PulsV*delSct	1021	713	0.095
EB*betLyr	945	900	0.12
S*	929	902	0.12
brownD*	914	886	0.12
BClG	846	834	0.11
IG	845	749	0.10
BLLac	735	705	0.094
Radio(mm)	692	67	0.0089
WD*	574	303	0.040
BYDra	552	526	0.070

Notes: a) Stars are counted separately because of their dominantly large number. b) Sign '*' denotes star; for example ** denotes the class of double or multiple star.

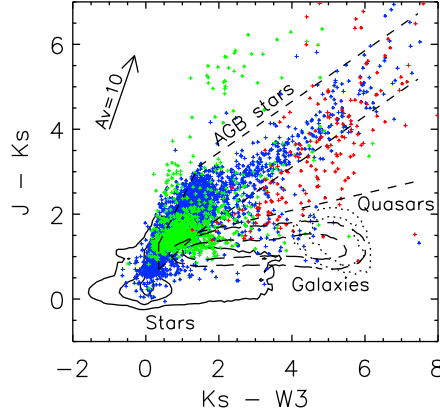


Fig. 2 $J - K_s$ versus $K_s - W3$ color-color diagram of the known C-rich and O-rich stars (blue: C-rich AGB stars; green: AGB stars; red: O-rich stars). The solid contours show 1-, 2-, and 3- σ regions of the normal stars, long-dashed contours 1- and 2- σ regions of the galaxies, and dotted contours 1- and 2- σ regions of the quasars. The dashed lines define the region for the AGB stars, although slightly contaminated by other sources. The direction of extinction is shown by the arrow.

Very approximate identification of the WISE sources can be conducted by directly constructing a color-color diagram (Wright et al., 2010). In order to as clearly as possible identify different classes of objects, we followed the method used by Ishihara et al. (2011). The WISE catalogue contains association information with the 2MASS All-Sky point source catalogue (Skrutskie et al., 2006), in which a $3''$ radius was used for determining the association. In order to be able to define classes of objects with sufficient color information, we selected those WISE sources that have association with one 2MASS source within $3''$ and were detected by all W1, W2, and W3 bands. We noted that to avoid ambiguous identification, 1.02 million WISE sources associated with more than one 2MASS sources were excluded in the selection. Because in general these 1.02 million sources have Galactic latitudes $gb < 20^\circ$, they are likely stars. Additionally excluding 6.23 million sources that are marked in any one of the WISE bands with a `cc_flag` of severe artifact contamination or confusion, we found that there are 76.10 million WISE sources that have both association with one 2MASS point source and the W1–W3 three band flux measurements.

2.2 SIMBAD Identifications

We input the positions of the 76 million WISE sources in the SIMBAD database and searched for class identifications with a search radius of $10''$. We found 3.4 million sources with identifications. Among them, 2.5 million are stars. In Table 1, we list the classes that have more than 500 SIMBAD-identified sources.

We carefully examined the distributions of position differences for these matches, since our search radius was $10''$ and this radius could cause false identifications, particularly at the Galactic plane. We found that for most of the classes, distribution peaks below $1''$ are clearly visible, likely indicating true matches between the WISE and SIMBAD sources. In Figure 1, the distributions of separation distances for the stars and carbon stars are shown as examples. For a comparison, the same distribution for the X-ray sources is also shown. It has a rising tail at distances greater than $2''$ and this tail is likely caused by positional coincidence when the density of sources is sufficiently high. We therefore rejected identifications greater than $2''$ radius away for every class of objects except high proper-motion stars.

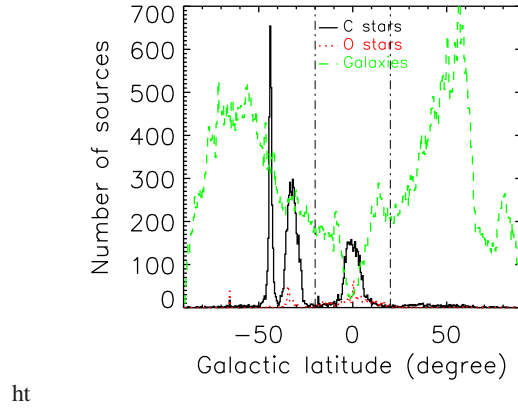


Fig. 3 A comparison of gb distributions of the AGB stars and that of the galaxies. The latter is scaled by 3 to clearly show the comparison. Large numbers of the known C-rich AGB stars in the LMC and SMC are clearly visible.

As also shown in Figure 1, their distribution peaks around $2''$, indicating proper motions between the epochs of previous observations of them in the SIMBAD database and the WISE observations. For them, we rejected those sources greater than $4''$ away. The numbers of different classes resulting from this criterion are given in column 3 of Table 1. The total number of them is 3.2 million, with 0.2 million excluded.

2.3 Color-Color Classification

We tested different ways of separating the AGB stars from the other sources, and found that the color-color diagram of $J - Ks$ versus $Ks - W3$ generally worked. In Figure 2 we show the diagram for the known AGB stars as well as contours that define the occupation regions for the stars and galaxies. As can be seen, the AGB stars are generally separated from the other sources, although a fraction of them are located in the region of the stars and slightly overlap with the blue end of the galaxy region. Because of the high density of the stars (Table 1), we defined the following three zones (zone 1, 2, and 3, respectively) that include most of the AGB stars while exclude the $2\text{-}\sigma$ contour regions of the stars and galaxies:

$$0.42 + 0.8 \times (Ks - W3) < (J - Ks) < 0.72 + 1.66 \times (Ks - W3) \text{ for } 0.35 < (Ks - W3) < 1.45, \quad (1)$$

$$0.71 + 0.6 \times (Ks - W3) < (J - Ks) < 2.25 + 0.6 \times (Ks - W3) \quad (2)$$

and

$$1.29 + 0.2 \times (Ks - W3) < (J - Ks) < 0.71 + 0.6 \times (Ks - W3) \text{ for } (Ks - W3) > 1.45. \quad (3)$$

We checked contamination by other classes of the sources, i.e., how many other sources are located in the three zones. The results are summarized in the second column of Table 2; only sources with relatively large numbers (> 500) are listed. It can be noted that because of large numbers of a few classes of objects (particularly the stars and galaxies), even a small fraction of them can be dominant over the targets. For example, there are approximately 4000 galaxies in the three zones. We therefore added one selection criterion based on source positions, requiring $|gb| \leq 20^\circ$. This constraint, estimated from the gb distributions of the sources, helped exclude most of extra-galactic sources including a large number of variable stars in the Large and Small Magellanic Clouds (LMC and SMC; see Figure 3). In

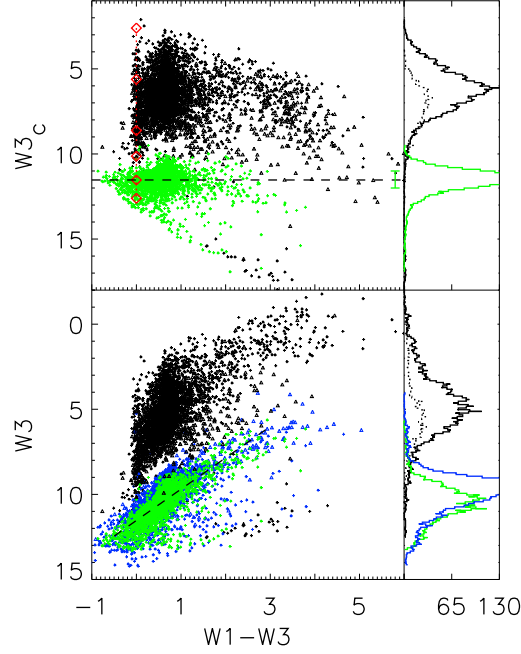


Fig. 4 *Bottom panels:* $W3$ versus $W1 - W3$ diagram of the C-rich and O-rich AGB stars in the Galaxy (black plus and triangle signs, respectively), LMC (blue plus and triangle signs), and SMC (green plus signs). The C-rich stars in the SMC can generally be represented by the dash line. The distributions of these stars as a function of $W3$ are respectively shown in the right narrow panel. *Top panels:* $W3_c$ versus $W1 - W3_c$ diagram of the same stars in the Galaxy and SMC. The red diamonds indicate distances of 1, 4, 16, 32, 61, and 100 kpc, estimated from $W3_c$ of the C-rich stars in the SMC (dashed line). The distributions of the stars are also shown in the right panel, which are sharpened compared to those in the bottom right panel. The green bar marks the standard deviation of 0.5 mag from $W3_c = 11.5$ of the AGB stars in the SMC.

addition, we noted that a large fraction of nearby stars, for example among the classes of the stars and proper motion stars, were also excluded. Adding this constraint, we re-calculated the numbers of the sources in the three zones and summarized the results in column 3 of Table 2.

2.4 WISE Color-Magnitude Analysis

The observed MIR fluxes and colors of an AGB star are generally determined by the interstellar extinction, mass loss rate of the star, and distance. Since the extinction is usually negligible at the MIR wavelengths (Indebetouw et al., 2005), the colors are a function of only the mass loss rate. A relation between values of one IR color and mass loss rates is often found when the mass loss rates can be obtained (e.g., Matsuura et al. 2009; Zhang et al. 2010; Ishihara et al. 2011). Also if considering that luminosities of AGB stars are similar, distances to them can be estimated (e.g., Le Bertre et al. 2001). We therefore checked the WISE color-magnitude diagram of the SIMBAD sample of the AGB stars (bottom left panel in Figure 4), in which we also included the known AGB stars in the LMC and SMC.

We found that the C-rich stars (few O-rich stars in the SMC were found in our sample; see, e.g., Marshall et al. 2004) in the SMC can generally be represented by a line in the diagram. Using

Table 2 Numbers of sources in the defined three zones of the AGB stars

Class	Total (All-sky)	Total ($ gb \leq 20^\circ$)	Zone 1	Zone 2	Zone 3	Total
Group A (same)						
IR	13194	12521	3022	2800	1481	7303
V*	8718	8408	4509	2044	1084	7637
Semi-regV*	8599	2409	1903	220	137	2260
Mira	3570	2244	1120	510	482	2112
Candidate_AGB*	2075	2070	0	803	304	1107
PulsV*	1467	1213	1084	39	26	1149
Group B (other)						
Star	9151	4976	3647	353	89	4089
Candidate_YSO	1759	1742	58	87	72	217
PM*	9351	1690	1021	1	0	1022
*inCl	1347	1033	553	24	7	584
Galaxy	3870	903	20	1	7	28
YSO	745	709	66	108	61	235
Group C (targeted)						
C*	8611	3259	2053	698	51	2802
AGB*	797	615	498	84	27	609
OH/IR	192	189	1	62	77	140
Fraction (%)						
C*	55	63	64	74	71	68
AGB*+OH/IR	53	68	62	84	93	71

Notes: Column 4–7 are the numbers of sources that additionally satisfy $W3_c \leq 11$.

a “robust” least absolute deviation method, we fit $W1-W3$ and $W3$ to a linear model and found $W3=11.53-1.83(W1-W3)$. This dependence on $W1-W3$ presumably reflects the mass loss rates of the stars and can probably be removed by defining a “corrected” magnitude $W3_c = W3+1.83(W1-W3)$. In the top left panel of Figure 4, we show the $W1-W3$ and $W3_c$ color-magnitude diagram of the AGB stars in the Galaxy and SMC, and as can be seen, the distribution of most SMC stars now is corrected to be horizontally elongated, with the central $W3_c$ value likely indicating the distance to the SMC and the spread of $W3_c$ values the depth of the SMC and probably the differences in the mass loss rates as well. We therefore used a distance of 61 kpc to the SMC (Lagadec et al., 2007) and derived the corresponding distance based on $W3_c$, and found most of the AGB stars in the Galaxy were in a range of 4–16 kpc (Figure 4). There are a few outliers in our sample of the Galactic AGB stars that have $W3_c > 15$, which are probably the AGB stars found in nearby dwarf galaxies by the previous surveys. As a check of our distance estimate method, we searched the C-rich and O-rich stars reported in Le Bertre et al. (2003) in the WISE catalogue and found 108 and 113 of them, respectively. The distances to these stars were estimated by Le Bertre et al. (2003), with a factor of 2 uncertainty. Their values were compared with that derived from our method, and 68% (1σ) of the 221 stars are consistent within 40%. The comparison result indicates that $W3_c$ can be used to estimate distances to AGB stars, although we cautiously note that the “systematic” uncertainty of the distances given by Le Bertre et al. (2003) is large and we have assumed that the intrinsic properties of the AGB stars through the WISE bands in the Galaxy and SMC are very similar.

From the above analysis, an additional criterion for selecting AGB stars in the Galaxy can be set. As shown in Figure 4, more than 80% of the AGB stars in the Galaxy have $W3_c \leq 11$ (or distance less than 50 kpc). Thus by requiring $W3_c \leq 11$, we further significantly reduced contamination from galaxies and excluded stars that are not located in our Galaxy. The results are summarized in column 4–7 of Table 2.

Following Ishihara et al. (2011), we divided the classes listed in Table 2 into three groups: A) objects are classified as different categories, but can be considered as the same group of our targets; B) objects are classified as other categories; C) classified targeted objects. We estimated the reliability of

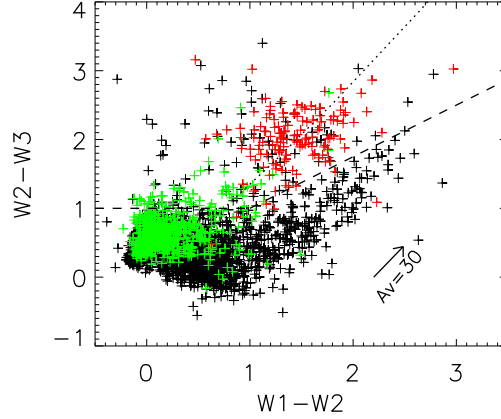


Fig. 5 WISE color-color diagram of the known C-rich stars (black), AGB stars (green), and OH/IR stars (red). The dotted curve indicates the colors for objects at different low temperatures (Wright et al., 2010), indicating that the OH/IR stars have temperatures 500–800 K. The dashed lines can generally separate the OH/IR and a small fraction of the AGB stars from the C-rich stars in our sample.

our classification using $(n_a + n_c)/(n_a + n_b + n_c)$. In group A, IR and variable stars were included as n_a for both C-rich and O-rich stars, while Mira and candidate AGB stars were included only as O-rich stars. The AGB and OH/IR stars were combined together as O-rich stars (Ishihara et al., 2011). The results are given in Table 2. The reliabilities for the C-rich and O-rich stars satisfying all the selecting criteria are 68% and 71%, respectively.

2.5 WISE Color-Color Separation Between C-Rich and O-Rich Stars

We investigated different combinations of WISE band color-color analyses for the purpose of separating C-rich and O-rich stars, and did not find a method that can clearly discriminate between the two sets of the stars. However as shown in Figure 5, which is the WISE $W2-W3$ versus $W1-W2$ diagram of the known C-rich and O-rich stars in our sample, the stars with extremely red colors can generally be defined. The conditions $W2-W3 > 1$ for $W1-W2 < 1$ and $W2-W3 \geq 0.75(W1-W2)+1$ for $W1-W2 \geq 1$ can also separate the OH/IR stars and a small fraction of the AGB stars from the C-rich stars in our sample.

3 RESULTS

Applying the IR color-color, Galactic latitude, $W3_c \leq 11$ selection criteria we have established to the 76 million WISE+2MASS sources, we searched for candidate AGB stars and found 1.37 million sources satisfying the three criteria, with 1.16, 0.189, and 0.025 million sources in the zone 1, 2, and 3, respectively. The distributions of the selected sources in the three zones as a function of $W3$ are shown in Figure 6. In addition, the same distribution for all 76 million sources is also shown in the figure. As can be seen, different from the distribution of the 76 million sources, there appear to have two components in both the zone 1 and 2 distributions. We noted that for the zone 1 sources, the upper edge of the main peak (at $W3=10$) was caused by the requirement of $W3_c \leq 11$. On the basis of the known AGB stars in the SMC, $W3_c \approx 11.53$ or $W3 \approx 11.53 - 1.83(W1-W3)$. Most AGB stars in the Galaxy and SMC have $W1-W3$ colors of 0–1 mag (Figure 4), implying a range of 5.3–7.2 mag for 8 kpc distance or 3.8–8.6

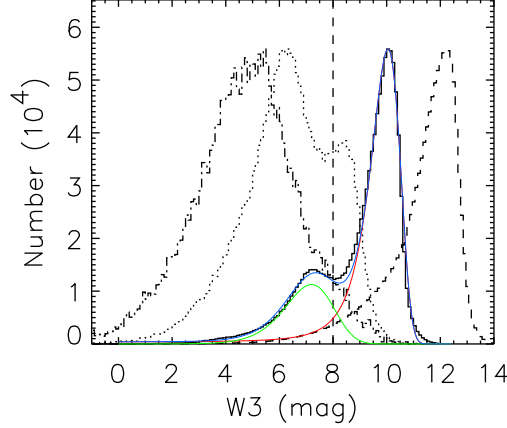


Fig. 6 Distributions of the candidate AGB stars in the zones 1 (solid curve), 2 (dotted curve), and 3 (dash-dotted curve) and 76 million WISE sources (dashed curve) as a function of W3. The distributions of the latter 3 were respectively scaled to best show the comparisons among them. Two components are visible in the zone 1 and 2 curves with a boundary approximately at 8 mag. The two components can be well represented by a modified Gaussian function (green curve for the AGB component, red for the normal star component, and blue for the sum of the two in zone 1).

mag for 4–16 kpc distance. Therefore the components of faint sources in the zone 1 and 2 distributions ($W3 \geq 8$) are likely normal stars, not AGB stars.

Using $W3=8$ as an approximate boundary to separate between the candidate AGB stars and normal stars for the zone 1 and 2 sources, 0.295 and 0.151 million candidate AGB stars were obtained. Now including those in zone 3, the total number is 0.471 million (34% of the 1.37 million sources). We also tested to fit the two components in the distribution curves with a modified Gaussian function $y \sim \exp(-x^2/2\sigma^2)$, where x was set as a function of $\exp(W3)$, and the fitting results of the numbers of the candidate AGB stars and normal stars were consistent with that from simply using $W3=8$ as a separation boundary. It should be noted that while the fractions of two components can be more accurately estimated by fitting, the sources can not be accordingly separated.

In Table 2 we estimated that approximately 20% of the selected sources should belong to Group B, and most of which should be normal stars. Our study of the W3 distributions has shown that the fraction of normal stars is as high as 66%. This large difference was likely caused by the star sample in the SIMBAD database, whose distribution along W3 peaks at 10 mag. Comparing it to that of the 76 million sources (peaks at 12 mag, which corresponds to 0.5 mJy; Figure 6), a large fraction of stars that have $W3=10-12$ were not represented by the SIMBAD sample. This bias probably made the fraction of normal stars from our selection method significantly underestimated.

Galactic reddening towards each selected source was estimated using the dust map of the Galaxy (Schlegel et al., 1998) and the reddening laws for the WISE bands given from Weingartner & Draine (2001) and Li & Draine (2001) were used. The distances were estimated using dereddened $W3_c$ and their Galactocentric distances R_g and vertical distances from the Galactic plane Z_g were accordingly estimated as well (a distance of 8 kpc to the Galactic center was used; Gillessen et al. 2009). The distributions of the sources along R_g and in the R_g versus Z_g plane are shown in the left panel of Figure 7. As can be seen the 2σ contour of the distribution in the latter extends to $R_g \approx 45$ kpc and $Z_g \approx 7$ kpc, both unrealistically large, indicating the large fraction of normal stars in our selected candidate AGB stars. The distances of normal stars were largely over-estimated using $W3_c$. Reducing our total number of candidates by 66% by requiring $W3 \leq 8$, we re-plotted the distribution contours in Figure 7. The max-

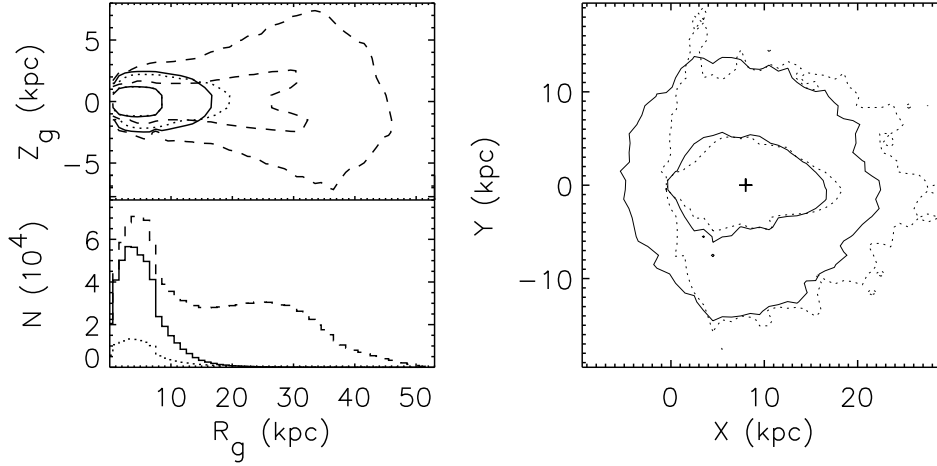


Fig. 7 Galactic distributions of the candidate AGB stars. *Top left:* 1- and 2- sigma contour regions (dashed curves) of the 1.37 million candidates. The solid and dotted contours show the same contours for the further selected 0.47 million candidates ($W3 \leq 8$) and for those candidate O-rich stars obtained from the WISE color-color analysis, respectively. *Bottom left:* Distributions of the total candidates (dashed), further selected candidates (solid), and those candidate O-rich stars (dotted) along the Galactocentric distance. *Right:* 1- and 2- σ distributions of the further selected candidate AGB stars (solid curves) and O-rich stars (dotted curves). The Sun is located at $X=0$, $Y=0$, and the Galactic center is marked by the plus sign.

imum R_g and Z_g values were changed approximately to 17 and 1 kpc, respectively. These values were significantly reduced and comparable to the typical size of the Galaxy. In the right panel of the figure, the distribution of the further selected candidate AGB stars projected onto the Galactic plane is shown. The candidates are generally distributed around the Galactic center.

Using the WISE color-color analysis given in Section 2.5, we searched for candidate O-rich stars among the 0.471 million candidates and found 0.119 million. The distributions of these 0.119 million sources are shown in Figure 7, and no significant differences between them and those of the other candidates are seen. This suggests that we probably did not select O-rich stars successfully, given that the currently known O-rich AGB stars appear to concentrate towards the Galactic center (Ishihara et al., 2011). The result is expected because as discussed in Ishihara et al. (2011), only the AKARI 9 and 18 μm bands well covered the silicate features of O-rich stars and clearly distinguished between O-rich and C-rich stars.

4 DISCUSSION

We analyzed the data in the newly released WISE all-sky source catalogue to search for C-rich and O-rich AGB stars in the Galaxy. We selected 76 million point sources in the catalogue that were detected in the first three WISE bands and have only one 2MASS counterpart within $3''$. A color-color diagram for these WISE+2MASS sources was constructed and occupation zones in the diagram for AGB stars were defined. The spatial requirement of $|gb| \leq 20^\circ$ was established to help exclude extra-galactic sources. Based on the known AGB stars in the Small Magellanic Cloud, we also derived “corrected” WISE third-band magnitudes $W3_c$ to estimate distances for AGB stars and to select candidates. Applying the color-color, spatial, and $W3_c$ criteria, 1.37 million candidates were selected. Analyses of them have showed that $W3 \leq 8$ was further required to separate the AGB stars from the normal stars in the candidates. As a result, 0.47 million candidate AGB stars were found, with their distances estimated and distributions in

the Galaxy obtained. Given the sensitivities of the WISE survey, which are an order of magnitude deeper than the MIR brightnesses expected for AGB stars in the Galaxy, these candidates probably constitute a large fraction of them. Observations of them are warranted for verifications.

In order to determine their AGB nature for the candidates, MIR spectroscopy best serves the purpose since the continuum of such a spectrum contains information about the mass loss rate of a target and the spectral features help directly identify whether it is a C-rich or O-rich star (Kraemer et al., 2002; Sloan et al., 2003). Currently only the Stratospheric Observatory for Infrared Astronomy (SOFIA) is operating at MIR wavelengths with spectroscopy capability, while a few large ground-based telescopes can reach a sensitivity of ~ 10 mJy at the wavelengths. However, neither is suitable for a spectroscopic survey of 0.5 million sources.

We note that strong optical spectral features arise from carbon-rich molecules (such as CN, C₂, and CH; Barnbaum et al. 1996) and C-rich stars can be identified from optical spectroscopy. The AGB stars in the SIMBAD database has a $V - K$ distribution with the peak at $V - K \approx 7$ and the Ks distribution of our 0.47 million candidates peaks at $Ks \sim 8$. Most of our candidates thus could have $V \sim 15$. Including reddening, the candidates are good targets for the Large Sky Area Multi-Object Fibre Spectroscopy Telescope (LAMOST) of China, which will start operation from the fall of 2012.

Acknowledgements This work was supported in part by the Pre-phase Studies of Space Science Projects of the Chinese Academy of Sciences, the National Natural Science Foundation of China (NSFC) under No.11073042, and National Basic Research Program of China (973 Project 2009CB824800). ZW is a Research Fellow of the One-Hundred-Talents project of Chinese Academy of Sciences.

This publication makes use of data products from the Wide-field Infrared Survey Explorer, which is a joint project of the University of California, Los Angeles, and the Jet Propulsion Laboratory/California Institute of Technology, funded by the National Aeronautics and Space Administration.

References

- Barnbaum, C., Stone, R. P. S., & Keenan, P. C. 1996, *ApJS*, 105, 419
 Gillessen, S., Eisenhauer, F., Trippe, S., Alexander, T., Genzel, R., Martins, F., & Ott, T. 2009, *ApJ*, 692, 1075
 Herwig, F. 2005, *ARA&A*, 43, 435
 Indebetouw, R., et al. 2005, *ApJ*, 619, 931
 Ishihara, D., Kaneda, H., Onaka, T., Ita, Y., Matsuura, M., & Matsunaga, N. 2011, *A&A*, 534, A79
 Kraemer, K. E., Sloan, G. C., Price, S. D., & Walker, H. J. 2002, *ApJS*, 140, 389
 Lagadec, E., et al. 2007, *MNRAS*, 376, 1270
 Le Bertre, T., Matsuura, M., Winters, J. M., Murakami, H., Yamamura, I., Freund, M., & Tanaka, M. 2001, *A&A*, 376, 997
 Le Bertre, T., Tanaka, M., Yamamura, I., & Murakami, H. 2003, *A&A*, 403, 943
 Li, A., & Draine, B. T. 2001, *ApJ*, 554, 778
 Marshall, J. R., van Loon, J. T., Matsuura, M., Wood, P. R., Zijlstra, A. A., & Whitelock, P. A. 2004, *MNRAS*, 355, 1348
 Matsuura, M., et al. 2009, *MNRAS*, 396, 918
 Murakami, H., et al. 2007, *PASJ*, 59, 369
 Schlegel, D. J., Finkbeiner, D. P., & Davis, M. 1998, *ApJ*, 500, 525
 Skrutskie, M. F., et al. 2006, *AJ*, 131, 1163
 Sloan, G. C., Kraemer, K. E., Price, S. D., & Shipman, R. F. 2003, *ApJS*, 147, 379
 Weingartner, J. C., & Draine, B. T. 2001, *ApJ*, 548, 296
 Wright, E. L., et al. 2010, *AJ*, 140, 1868
 Zhang, H.-J., Zhou, J.-J., Dong, G.-L., Esimbek, J., & Mu, J.-M. 2010, *Ap&SS*, 330, 23